THE JOURNAL OF BIOLOGICAL CHEMISTRY VOL. 292, NO. 8, pp. 3213–3223, February 24, 2017


# The Activating C-type Lectin-like Receptor NKp65 Signals through a Hemi-immunoreceptor Tyrosine-based Activation Motif (hemITAM) and Spleen Tyrosine Kinase (Syk)*

Received for publication, September 23, 2016, and in revised form, January 11, 2017 Published, JBC Papers in Press, January 12, 2017, DOI 10.1074/jbc.M116.759977

**Björn Bauer, Tanja Wotapek, Tobias Zöller, Emilia Rutkowski, and Alexander Steinle**[1]

*From the Institute for Molecular Medicine, Goethe University, 60590 Frankfurt am Main, Germany*

**Edited by Luke O'Neill**

**NKp65 is an activating human C-type lectin-like receptor (CTLR) triggering cellular cytotoxicity and cytokine secretion upon high-affinity interaction with the cognate CTLR keratinocyte-associated C-type lectin (KACL) selectively expressed by human keratinocytes. Previously, we demonstrated that NKp65-mediated cellular cytotoxicity depends on tyrosine 7, located in a cytoplasmic sequence motif of NKp65 resembling a hemi-immunoreceptor tyrosine-based activation motif (hemITAM). HemITAMs have been reported for a few activating myeloid-specific CTLRs, including Dectin-1 and CLEC-2, and consist of a single tyrosine signaling unit preceded by a triacidic motif. Upon receptor engagement, the hemITAM undergoes phosphotyrosinylation and specifically recruits spleen tyrosine kinase (Syk), initiating cellular activation. In this study, we addressed the functionality of the putative hemITAM of NKp65. We show that NKp65 forms homodimers and is phosphorylated at the hemITAM-embedded tyrosine 7 upon engagement by antibodies or KACL homodimers. HemITAM phosphotyrosinylation initiates a signaling pathway involving and depending on Syk, leading to cellular activation and natural killer (NK) cell degranulation. However, although NKp65 utilizes Syk for NK cell activation, a physical association of Syk with the NKp65 hemITAM could not be detected, unlike shown previously for the hemITAM of myeloid CTLR. Failure of NKp65 to recruit Syk is not due to an alteration of the triacidic motif, which rather affects the efficiency of hemITAM phosphotyrosinylation. In summary, NKp65 utilizes a hemITAM-like motif for cellular activation that requires Syk, although Syk appears not to be recruited to NKp65.**

The immune system employs a plethora of cell types that orchestrate an immune response to pathogens and malignant cells threatening the integrity of an organism. Mammalian immune cells are categorized into cells of the adaptive branch, namely T and B lymphocytes, characterized by the generation of antigen-specific receptors through somatic gene rearrangement, and innate immune cells. The latter solely utilize germ line-encoded receptors to recognize "threats" to the organism. These include innate lymphocytes, comprising cytotoxic natural killer (NK)[2] cells, and non-cytotoxic innate lymphoid cells (ILCs). ILCs are currently divided into three groups according to their cytokines produced: ILC1s secrete type 1 cytokines such as IFNγ and TNF, ILC2s produce type 2 cytokines such as IL-4 and IL-13, and ILC3s secrete Th17 cytokines such as IL-17 and IL-22 (1, 2). NK cells not only secrete type 1 cytokines but also exert cellular cytotoxicity to eradicate malignantly transformed or virally infected cells and to regulate immune responses (3, 4).

Many human NK cell receptors activating cytotoxicity belong either to the Ig-like superfamily, such as the natural cytotoxicity receptors NKp46, NKp44, and NKp30, or to the C-type lectin-like superfamily. These NK-related C-type lectin-like receptors (CTLRs) are encoded in the human natural killer gene complex on chromosome 12 (5–7) and are dimeric type II transmembrane glycoproteins with a single C-type lectin-like ectodomain. They include CD94/NKG2x receptors, NKG2D, and the NKRP1 receptors NKR-P1A (CD161), NKp80, and NKp65. Although NKR-P1A inhibits the effector functions of human NK cells (8, 9), NKp80 and NKp65 activate NK cells (10–12). NKp80 is expressed on all peripheral blood NK cells and binds to AICL, an adjacently encoded CTLR (11). AICL is up-regulated on activated monocytes and NK cells, thereby facilitating NK-monocyte cross-talk and immune control of activated NK cells (11, 13). NKp65, a close relative of NKp80, has so far only been found to be expressed on NK-92MI, a cell line isolated from an NK lymphoma (14). Of note, NKp65 binds with an exceptionally high affinity to KACL, a CTLR almost exclusively expressed on human keratinocytes (12, 15). The crystal structure of the $(sNKp65)_2$-$(sKACL)_2$ tetrameric complex shows a symmetrical, butterfly-shaped assembly with a high shape complementarity of the receptor-ligand interface, explaining the high affinity in the nanomolar range (16). This interface comprises several hot spot amino acid residues that crucially contribute to the tight interaction (16, 17).

* This work was supported by a grant of the Deutsche Forschungsgemeinschaft (DFG; STE 828/6-2) (to A. S.). A. S. holds a patent on NKp65.

[1] To whom correspondence should be addressed: Institute for Molecular Medicine, Goethe University, Theodor-Stern-Kai 7, 60590 Frankfurt am Main, Germany. Tel.: 49-69-6301-3700; Fax: 49-69-6301-7380; E-mail: alexander.steinle@kgu.de.

[2] The abbreviations used are: NK, natural killer; ILC, innate lymphoid cell; CTLR, C-type lectin-like receptor; AICL, activation-induced C-type lectin; KACL, keratinocyte-associated C-type lectin; ITAM, immunoreceptor tyrosine-based activation motif; hemITAM, hemi-immunoreceptor tyrosine-based activation motif; Syk, spleen tyrosine kinase; PMA, phorbol 12-myristate 13-acetate; SH, Src homology; SPR, surface plasmon resonance; sNKp65, soluble NKp65; sKACL, soluble KACL; SFK, Src family kinase; HBSS, Hanks' balanced salt solution; mAb, monoclonal antibody; pAb, polyclonal antibody; APC, allophycocyanin; PE, phycoerythrin.

Most activating immunoreceptors such as the T cell receptor (TCR) or natural cytotoxicity receptors associate with adaptor molecules such as CD3ζ or DAP12 bearing one or several immunoreceptor tyrosine-based activation motifs (ITAMs) consisting of two tyrosine modules. Upon ligand engagement, these tyrosine residues become phosphorylated by members of the Src kinase family and recruit the Syk family members Syk and/or ZAP-70, which, in turn, activate signaling components such as SLP-76, PLCγ, and Vav proteins (18, 19). In the case of cytotoxic lymphocytes, these signaling proteins initiate a complex process composed of actin reorganization, direction of cytolytic vesicles containing perforin and granzymes to the cell surface, and targeted release of their cytolytic content at the target cell interface, resulting in cellular cytotoxicity (20).

A signaling motif consisting of only one tyrosine module, hence termed hemITAM, has been described for some myeloid-specific CTLRs such as CLEC-2 and Dectin-1 (21, 22). Upon ligand binding, the hemITAM is phosphorylated and recruits Syk, initiating cellular activation. Phosphorylation of the hemITAM tyrosine is dependent on an upstream triacidic motif and the activity of Src kinases (23). Syk has been shown to bridge two CLEC-2 homodimers via its tandem SH2 domains and to contribute to hemITAM phosphorylation (24, 25). It remains to be shown whether such a mechanism also applies to other hemITAM-bearing receptors. A more recent study suggested that CLEC-2 engagement activates Syk through a Src-PI3K-Tec pathway (26).

We recently reported that the NK receptor NKp80 also utilizes a hemITAM-like motif and Syk kinase for triggering cellular cytotoxicity (27, 28). However, unlike myeloid hemITAM, NKp80 does not recruit Syk kinase because of non-consensus amino acids directly preceding tyrosine 7 (28). Reconstitution of the hemITAM consensus strongly enhanced NKp80 hemITAM phosphorylation and allowed Syk recruitment (28). Such Syk recruitment was accompanied by a more potent functional response in terms of cytotoxicity and cytokine secretion. In contrast, other NKp80 mutants that showed increased hemITAM phosphorylation, but no Syk recruitment, did not exhibit a stronger functional response (28).

In our first report on NKp65, we showed that NKp65, in contrast to NKp80, potently triggers cellular cytotoxicity and cytokine secretion by NK-92MI cells (12). Cytotoxicity triggered by NKp65 strictly depends on tyrosine 7, which, in contrast to NKp80, is embedded in a nearly perfect hemITAM consensus sequence. Hence, we expected NKp65 to initiate cellular activation by recruitment and activation of Syk in our ensuing studies addressing NKp65 signaling.

## Results

*NKp65-mediated Cellular Activation Strictly Depends on Phosphorylation of the NKp65 hemITAM*—We have shown previously that NKp65 activates cellular cytotoxicity and cytokine secretion by NK-92MI cells (12). Using a redirected lysis assay and antibodies specific for carboxyl-terminal sequence tags added to NKp65, we have also shown that tyrosine 7 of NKp65 is required to trigger cytotoxicity (12). Well in line with these previous results, we now show, using the newly generated NKp65-specific mAb OMAR1, that antibody-mediated ligation of NKp65 triggers degranulation of NK-92MI cells, whereas ligation of an NKp65 mutant, where tyrosine 7 is replaced by phenylalanine (NKp65-Y7F), does not stimulate degranulation (Fig. 1*A*). Importantly, both NKp65 and NKp65-Y7F are expressed at comparable levels on the respective NK-92MI transductants (data not shown) and degranulate to a similar extent when generically activated with PMA and ionomycin (Fig. 1*A*). Similarly, antibody-mediated cross-linking of NKp65, but not of NKp65-Y7F, stimulated calcium influx into NK-92MI transductants (Fig. 1*B*), demonstrating that tyrosine 7 is strictly required for NKp65-mediated cellular activation. Tyrosine 7 is embedded in an amino-terminal cytoplasmic sequence motif of NKp65 that resembles a hemITAM described previously for some myeloid C-type lectin-like receptors such as Dectin-1, CLEC-2, and DNGR-1 (Fig. 1*C*) (21, 22, 29). Because hemITAM-mediated signaling is initiated by phosphorylation of the hemITAM-embedded tyrosine, we next addressed whether tyrosine 7 of NKp65 becomes phosphorylated upon NKp65 ligation.

Treatment of NK-92MI-NKp65 cells with the broad protein-tyrosine phosphatase inhibitor pervanadate resulted in substantial tyrosine phosphorylation of NKp65 (Fig. 1*D*). To assess whether tyrosine phosphorylation of NKp65 is also specifically induced upon NKp65 ligation, NKp65 on NK-92MI-NKp65 cells was cross-linked with mAb OMAR1. Tyrosine phosphorylation of NKp65 became clearly detectable ~30 s after cross-linking and subsequently increased further (Fig. 1*E*). In contrast, NKp65-Y7F was not phosphotyrosinylated upon cross-linking, well in line with the importance of tyrosine 7 phosphorylation for the functionality of the NKp65 hemITAM (Fig. 1*E*). Altogether, these data demonstrate that cellular activation by NKp65 occurs in a hemITAM-dependent manner.

*Syk Is Not Recruited by the NKp65 hemITAM but Crucially Involved in the NKp65 Signaling Pathway*—Typically, hemITAM-mediated signaling by myeloid CTLR includes the recruitment of Syk to the phosphorylated hemITAM (22). Because NKp65 shares the hemITAM consensus with these myeloid CTLRs (Fig. 1*C*) and potently activates effector functions of NK-92MI cells in a hemITAM-dependent manner, we expected NKp65 to recruit Syk upon activation.

To address an involvement of Syk in NKp65-mediated cellular activation, we monitored the degranulation of NK-92MI-NKp65 cells in the presence of a Syk inhibitor. Degranulation of NK-92MI-NKp65 cells upon NKp65 cross-linking by OMAR1 was inhibited by addition of Syk inhibitor IV in a concentration-dependent manner (Fig. 2*A*). In accord with this finding, antibody-mediated cross-linking of NKp65 led to a marked phosphorylation of Syk in NK-92MI cells (Fig. 2*B*). However, no Syk phosphorylation was observed when NKp65-Y7F was cross-linked, demonstrating that NKp65-induced phosphorylation of Syk depends on the presence of the hemITAM-embedded tyrosine 7.

Next we addressed Syk recruitment by the phosphorylated hemITAM of NKp65. To this aim, NK-92MI-NKp65 cells were treated with pervanadate to stimulate phosphorylation of tyrosine 7, followed by NKp65 immunoprecipitation and Syk immunoblotting. For comparison, NKp80 from pervanadate-

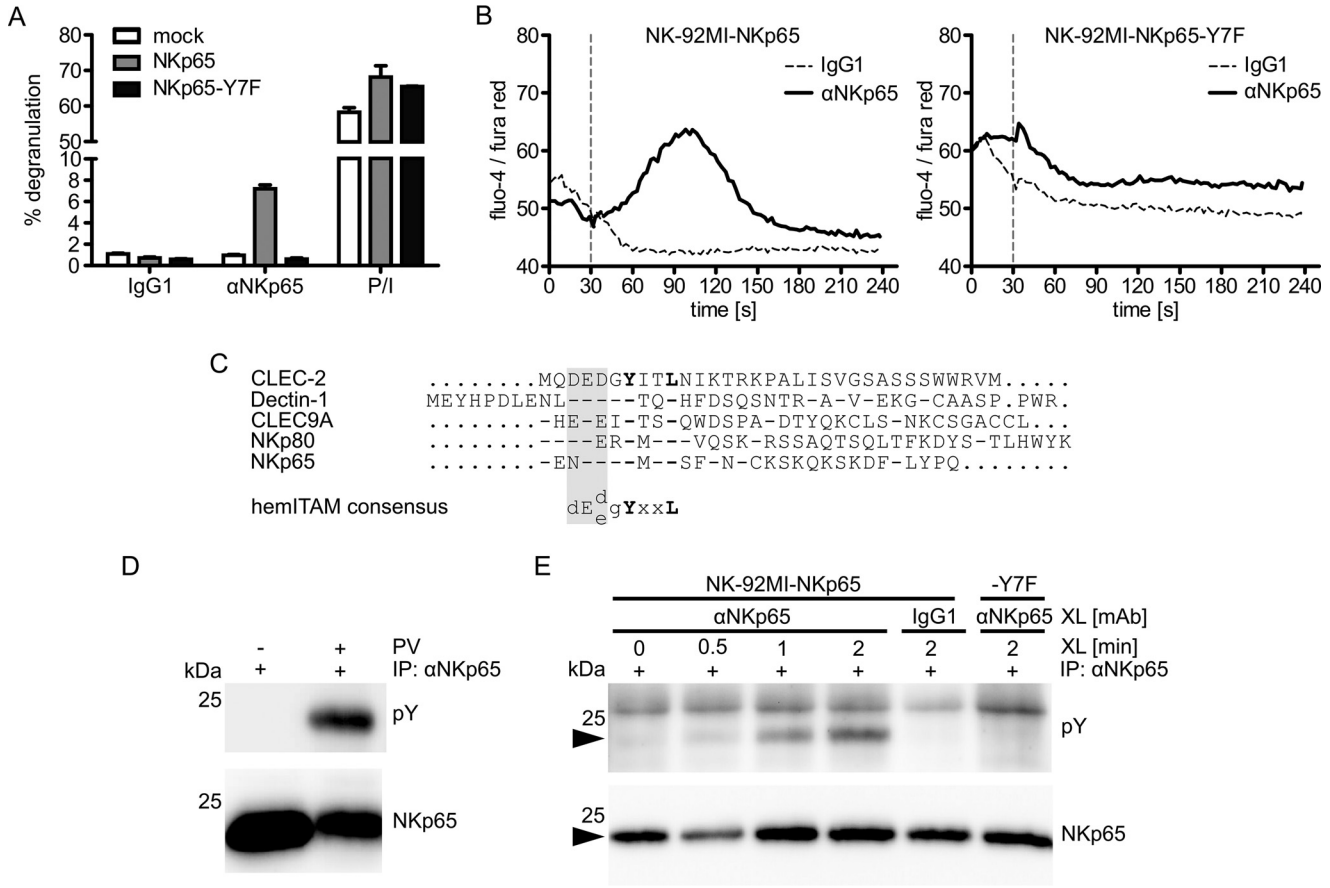


FIGURE 1. **Cellular activation by NKp65 requires phosphotyrosinylation of the NKp65 hemITAM.** *A*, degranulation of NK-92MI cells transduced with cDNA encoding for NKp65 or NKp65-Y7F or empty vector (*mock*) after 2-h co-culture with P815 loaded with the anti-NKp65 mAb OMAR1 or an irrelevant IgG1. For control, NK-92MI cells were treated with PMA plus ionomycin (*P/I*). The percentage of $CD107a^+$ NK-92MI cells is shown. Viable ($DAPI^-$) $CD56^+$ cells were gated for analysis by flow cytometry. Depicted are means ± S.D. of triplicates from one representative of at least three independent experiments. *B*, the calcium flux of NK-92MI-NKp65 or NK-92MI-NKp65-Y7F cells was assessed by flow cytometry upon NKp65 cross-linking. OMAR1 (*solid line*) or an irrelevant IgG1 (*dashed line*) was added to NK-92MI cells and, after baseline recording for 30 s, cross-linked by addition of anti-mouse IgG antibodies (*vertical dashed line*). The ratio of median fluorescence intensities (*fluo-4/fura red*) was recorded by flow cytometry as a function of time. One representative of three independent experiments is depicted. *C*, amino acid alignment of the cytoplasmic domains of hemITAM-bearing human CTLR. *Dashes* indicate identical amino acids, and *dots* represent sequence gaps. The hemITAM comprises a triacidic sequence (*shaded*) preceding the strictly conserved *YXX*L module. *D*, NK-92MI-NKp65 cells were treated with or without pervanadate (*PV*) at 37 °C for 3 min. FLAG-tagged NKp65 was immunoprecipitated (*IP*) with OMAR1 and probed with the anti-phosphotyrosine mAb 4G10 (Tyr(P)) in immunoblotting. The membrane was reprobed with the anti-FLAG mAb M2 for control. *E*, NK-92MI-NKp65 or NK-92MI-NKp65-Y7F cells preloaded with OMAR1 were incubated for the indicated times at 37 °C with anti-mouse IgG antibodies to achieve NKp65 cross-linking (*XL*) and subsequently lysed. NKp65 immunoprecipitation and immunoblotting were performed as in *D*. For control, NK-92MI-NKp65 cells were preloaded with irrelevant IgG1. Depicted is one representative of four independent experiments. The position on NKp65 is marked by *arrowheads*.

treated NK-92MI-NKp80 or NK-92MI-NKp80-DG cells was immunoprecipitated. We have reported previously that the hemITAM of NKp80 does not recruit Syk because of the presence of two non-consensus amino acids (glutamic acid 5 and arginine 6) directly preceding tyrosine 7 (28). Accordingly, an NKp80 mutant with a reconstitution of the hemITAM consensus (NKp80-DG) regained the capacity to recruit Syk (28).

Well in line with our previous results, Syk was detectable in precipitates of NKp80-DG (Fig. 2*C*). However, Syk was not detectable in precipitates of both phosphotyrosinylated NKp65 and NKp80, strongly suggesting that NKp65, much like NKp80, does not recruit Syk (Fig. 2*C*). Syk recruitment to other hemITAM receptors such as CLEC-2 was assessed by GST pull-down experiments by using the tandem SH2 domain of Syk fused to GST (21, 30). Therefore, we re-enacted the GST pull-down by immobilizing purified GST-Syk-SH2 fusion protein on glutathione-agarose and incubation with NKp65, NKp65-Y7F, NKp80-DG, and NKp80 enriched from pervanadate-treated NK-92MI cells by anti-FLAG immunoprecipitation (Fig. 2*D*). GST-Syk-SH2 only pulled down NKp80-DG but not NKp65, NKp65-Y7F, or NKp80, thereby confirming the results above from immunoprecipitations and revealing a critical difference of both NKp65 and NKp80 from CLEC-2, which was successfully pulled down by this strategy (21, 30). Hence, triggering of cytotoxicity via NKp65 involves and depends on Syk activation, which, in turn, depends on a functional NKp65 hemITAM. However, in contrast to hemITAM-bearing myeloid CTLR, NKp65 apparently does not recruit Syk via its hemITAM.

*The Altered Triacidic Motif of the NKp65 hemITAM Impairs hemITAM Phosphorylation but Not Cellular Activation or Syk Recruitment*—The observed failure of NKp65 to recruit Syk was unexpected, as the NKp65 hemITAM conforms to the hemITAM consensus (Fig. 1*C*). Just the exchange of aspartic acid for asparagine at position 3 slightly deviates from the

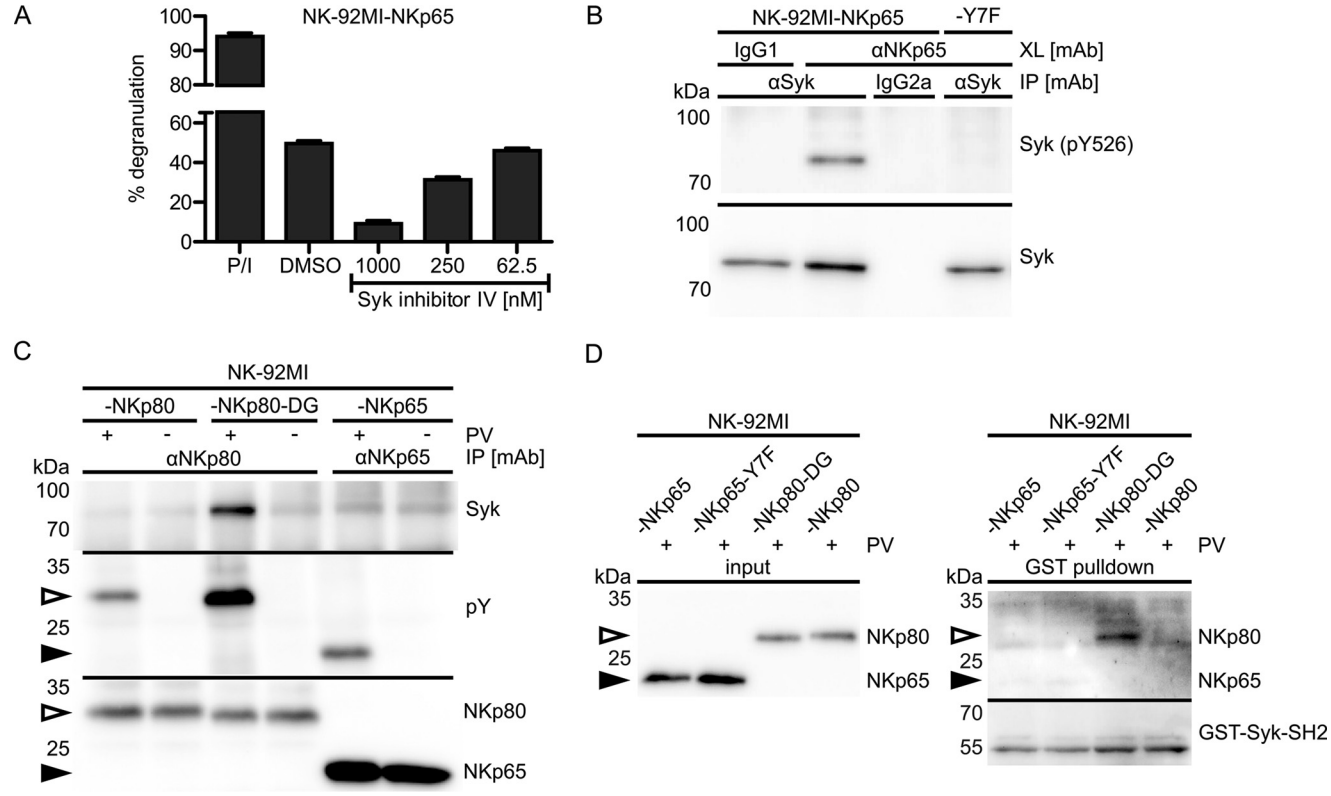


FIGURE 2. **NKp65 triggers degranulation in a Syk-dependent manner and stimulates Syk phosphotyrosinylation but does not recruit Syk.** *A*, degranulation of NK-92MI-NKp65 cells after 2-h co-culture with P815 loaded with the anti-NKp65 mAb OMAR1 in the presence of the indicated concentrations of Syk inhibitor IV or DMSO (vehicle control). For control, NK-92MI cells were treated with PMA plus ionomycin (*P/I*). The percentage of CD107a$^+$ NK-92MI cells is shown. Viable (DAPI$^-$) CD56$^+$ cells were gated for analysis by flow cytometry. Depicted are means ± S.D. of triplicates from one representative of two independent experiments. *B*, Syk phosphotyrosinylation upon NKp65 cross-linking (*XL*). NKp65 on NK-92MI-NKp65 or NK-92MI-NKp65-Y7F cells was cross-linked for 2 min with OMAR1 and secondary anti-mouse IgG antibodies. Syk was immunoprecipitated (*IP*) from cellular lysates with anti-Syk mAb (4D10.2) and probed with anti-phosphotyrosine (Tyr(P)-526) Syk pAb (2710) by immunoblotting and for control with anti-Syk pAb (2712). For control, irrelevant mouse IgG1 was added to cells instead of OMAR1. Irrelevant mouse IgG2a was used for control of specificity of Syk immunoprecipitation. Depicted is one representative of two independent experiments. *C*, NK-92MI-NKp80, NK-92MI-NKp80-DG, or NK-92MI-NKp65 cells were treated with or without pervanadate (*PV*) at 37 °C for 5 min. Subsequently, NKp80 and NKp80-DG were immunoprecipitated with the anti-NKp80 mAb 5D12 and NKp65 with OMAR1, respectively. Immunoprecipitates were probed for the presence of Syk with mAb 4D10.2 (*top*) and for phosphotyrosinylation of NKp80, NKp80-DG, and NKp65, respectively, with the anti-phosphotyrosine mAb P-100 (*center*). Successful immunoprecipitation of FLAG-tagged NKp80, NKp80-DG (*open arrowheads*), and NKp65 (*filled arrowheads*), respectively, was monitored by reprobing the membrane with anti-FLAG (M2) and anti-NKp80 sheep pAb (*bottom*). Depicted is one representative of three independent experiments. *D*, GST-Syk-SH2 pulldown. The tandem SH2 domains of Syk were fused to GST and immobilized on glutathione-agarose. NK-92MI-NKp65, NK-92MI-NKp65-Y7F, NK-92MI-NKp80-DG, or NK-92MI-NKp80 cells were treated for 5 min with pervanadate, followed by enrichment of NKp65, NKp65-Y7F, NKp80-DG, and NKp80 by immunoprecipitation with anti-FLAG (M2)-coated magnetic beads and elution with FLAG peptides. Enriched receptors were incubated with GST-Syk-SH2-loaded agarose. After washing, proteins were eluted and deglycosylated with PNGase F. Eluates were probed for the presence of NKp65 and NKp80 with anti-FLAG (M2) and anti-NKp80 sheep pAb (*top*). For control, the membrane was reprobed with anti-GST mAb (*bottom*).

hemITAM consensus, altering the triacidic motif (Fig. 1*C*) (23). This specific deviation from an otherwise matched hemITAM consensus also occurs in the NKp65 sequences of many other mammalian species, indicating an evolutionary conserved function (Fig. 3*A*).

Hence, we figured that asparagine 3, in the absence of any other obvious mismatch, may account for the impaired Syk recruitment. To test this presumption, we reconstituted the triacidic motif by replacing asparagine 3 with aspartic acid (NKp65-N3D). NKp65-N3D was expressed on NK-92MI transductants at levels comparable with NKp65 and NKp65-Y7F, respectively (data not shown). Subsequent to antibody-mediated cross-linking, NKp65-N3D was immunoprecipitated from NK-92MI-NKp65-N3D cells and assayed for phosphorylation and Syk recruitment. Tyrosine phosphorylation was detected for NKp65-N3D as well as for NKp65 but not for NKp65-Y7F, confirming previous results. Interestingly, phosphorylation of NKp65-N3D was substantially enhanced compared with NKp65 (Fig. 3*B*). However, Syk remained undetectable in NKp65-N3D precipitates, rejecting the notion that impaired Syk recruitment may be due to the alteration of the triacidic motif (Fig. 3, *B* and *C*).

To address the possibility that NKp65 endogenously expressed in NK-92MI cells (12) may dimerize with the transduced NKp65-N3D and thereby block Syk recruitment in a dominant negative manner, we transduced NKp65-negative Jurkat cells with NKp65-N3D as well as with NKp65, NKp65-Y7F, and NKp80-DG, respectively. Subsequent to antibody-mediated cross-linking and immunoprecipitation of the transduced receptors, precipitates were analyzed by immunoblotting (Fig. 3*D*). Both NKp65 and NKp65-N3D, but not NKp65-Y7F, were phosphotyrosinylated, with NKp65-N3D again showing enhanced phosphorylation compared with NKp65. However, Syk was not co-immunoprecipitated by

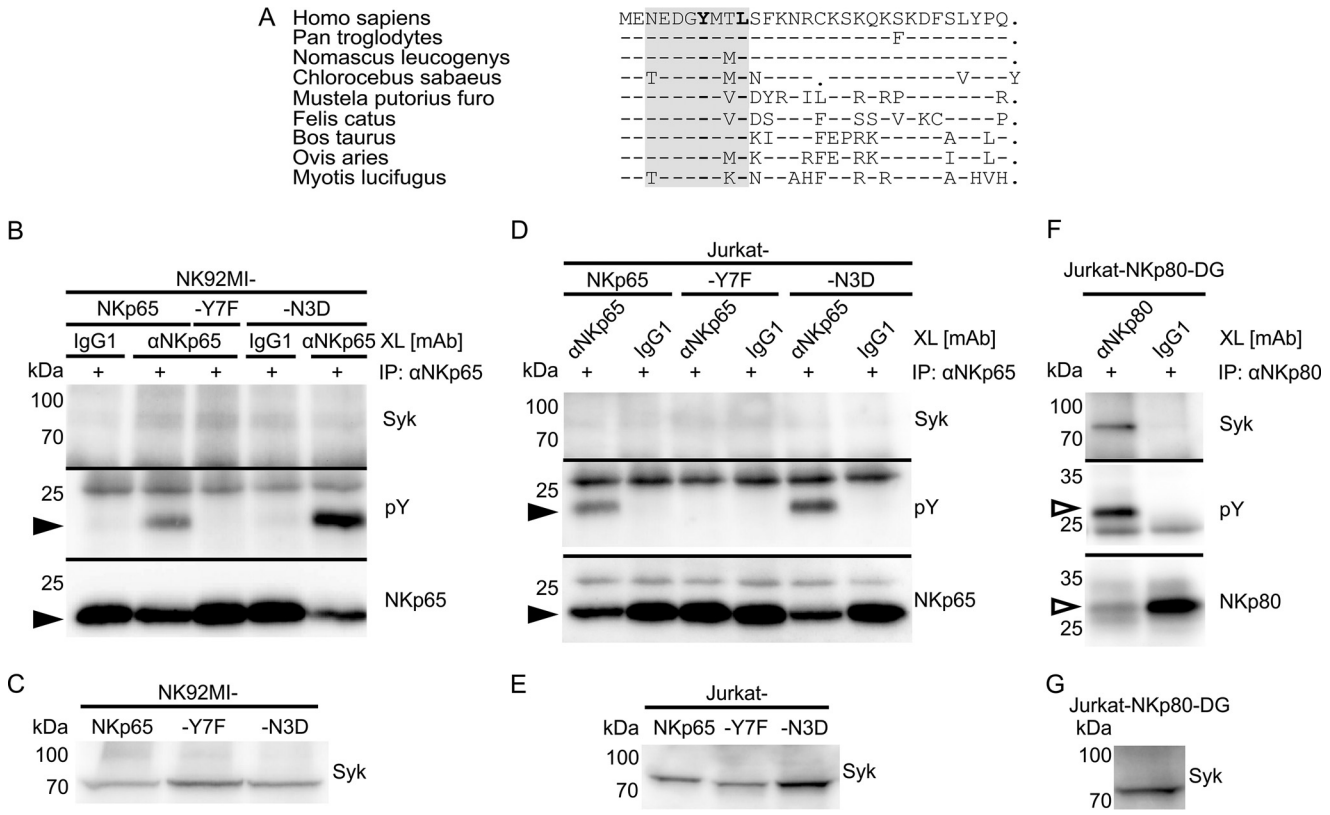


FIGURE 3. **The altered triacidic motif of the NKp65 hemITAM impairs NKp65 phosphotyrosinylation but does not account for the deficient Syk recruitment.** *A*, amino acid sequence alignment of the cytoplasmic amino acids of NKp65 from the indicated mammalian species. *Dashes* indicate identical amino acids, and *dots* represent sequence gaps. The hemITAM is *shaded*. *B*, NKp65 on NK-92MI-NKp65, NK-92MI-NKp65-Y7F, or NK-92MI-NKp65-N3D cells was cross-linked (*XL*) with OMAR1 and secondary anti-mouse IgG antibodies for 2 min at 37 °C. For control, irrelevant mouse IgG1 was added instead of OMAR1. Subsequently, NKp65 was immunoprecipitated (*IP*) from cellular lysates with OMAR1, and immunoprecipitates were probed for the presence of Syk with mAb 4D10.2 (*top*) and for phosphotyrosinylation of NKp65 with the anti-phosphotyrosine mAb 4G10 (*center*). Successful immunoprecipitation of NKp65 was monitored by reprobing the membrane with anti-FLAG (M2) (*bottom*). Depicted is one representative of four independent experiments. *C*, immunoblotting of cellular lysates of NK-92MI-NKp65, NK-92MI-NKp65-Y7F, or NK-92MI-NKp65-N3D cells with mAb 4D10.2 reveals comparable Syk expression. *D* and *F*, NKp65 on Jurkat-NKp65, Jurkat-NKp65-Y7F, or Jurkat-NKp65-N3D cells was cross-linked with OMAR1 as in *B*. NKp80 on Jurkat-NKp80-DG cells was cross-linked with the anti-NKp80 mAb 5D12. For control, irrelevant mouse IgG1 was added instead. NKp65 and NKp80 were immunoprecipitated from lysates with OMAR1 and 5D12, respectively, and immunoprecipitates were analyzed by immunoblotting as in *B*, except that the mAb P-100 was used to detect phosphotyrosinylated NKp80 and anti-NKp80 sheep antibodies to monitor efficient NKp80 immunoprecipitation. *E* and *G*, immunoblotting of cellular lysates of Jurkat-NKp65, Jurkat-NKp65-Y7F, Jurkat-NKp65-N3D, or Jurkat-NKp80-DG cells with mAb 4D10.2 reveals comparable Syk expression. *B*, *D*, and *F*, *filled* and *unfilled arrowheads* mark the positions of NKp65 and NKp80-DG, respectively.

NKp65 or NKp65-N3D (Fig. 3, *D* and *E*) but by NKp80-DG (Fig. 3, *F* and *G*), in line with previous results.

To address the impact of the altered triacidic motif on the functional capacity of NKp65, we assessed degranulation of NK-92MI-NKp65 *versus* NK-92MI-NKp65-N3D cells in co-cultures with anti-NKp65-loaded P815 cells. The extent of NKp65-N3D-stimulated degranulation did not significantly differ from NKp65-stimulated degranulation, with both transductants similarly responding to receptor-independent activation by PMA/ionomycin treatment (Fig. 4*A*). Accordingly, antibody-mediated cross-linking of NKp65 and NKp65-N3D similarly evoked a calcium influx in NK-92MI cells (Fig. 4*B*). However, the NKp65-triggered calcium flux in Jurkat cells was time-delayed as compared with NK-92MI cells, with the NKp65-N3D-induced influx being apparently stronger (Fig. 4*C*). In contrast, the NKp80-DG-triggered calcium influx in Jurkat cells was immediate and strong, in line with the more potent signaling of a Syk-recruiting hemITAM (Fig. 4*C*). Altogether, these data show that the modified triacidic motif of NKp65 affects NKp65 hemITAM phosphorylation but has no major impact on Syk recruitment.

*Engagement of Homodimeric NKp65 by KACL Results in Tyrosine Phosphorylation but Not Syk Recruitment*—Having ruled out that failure to recruit Syk by NKp65 is due to a sequence deviation from the hemITAM consensus, we considered the possibility that Syk recruitment by NKp65 may require KACL-induced homodimerization and/or conformational changes that may not be elicited by antibody-mediated NKp65 cross-linking. This idea was nurtured by the claim originating from structural studies that NKp65 occurs in a monomeric form and that engagement by a KACL homodimer is required to dimerize NKp65 for subsequent signaling (16). Li *et al.* (16) did not detect a homodimerization interface in the crystal structure of the NKp65-KACL complex and concluded that NKp65 exists as a monomer. To address a monomeric *versus* dimeric state of NKp65, we subjected sNKp65 to size exclusion chromatography. The elution profile of soluble NKp65 (sNKp65) indicated a molecular mass of ~50 kDa, corresponding to the calculated mass of an sNKp65 homodimer (Fig. 5, *A* and *B*). Similarly, the elution profiles of sNKp80 and sKACL corresponded to the calculated masses of the respective homodimers (Fig. 5, *A* and *B*). A complex of higher molecular

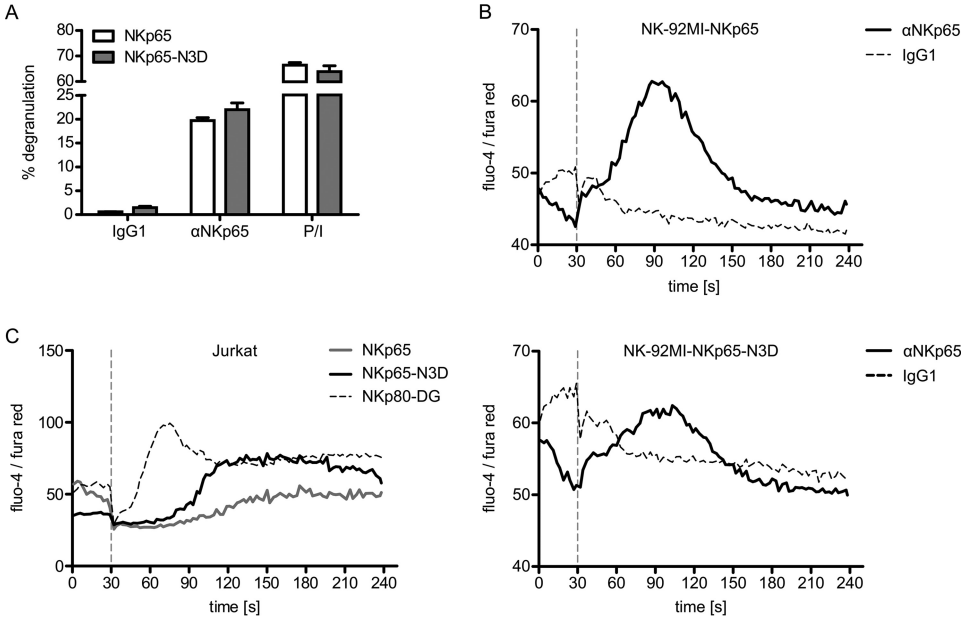


FIGURE 4. **The altered triacidic motif within the NKp65 hemITAM does not affect cellular activation.** *A*, degranulation of NK-92MI-NKp65 or NK-92MI-NKp65-N3D cells after 2-h co-culture with P815 loaded with the anti-NKp65 mAb OMAR1. For control, NK-92MI cells were treated with PMA plus ionomycin (*P/I*). The percentage of $CD107a^+$ NK-92MI cells is shown. Viable ($DAPI^-$) $CD56^+$ cells were gated for analysis by flow cytometry. Depicted are the means ± S.D. of triplicates from one representative of at least three independent experiments. *B*, the calcium flux of NK-92MI-NKp65 (*top panel*) or NK-92MI-NKp65-N3D cells (*bottom panel*) was assessed by flow cytometry upon NKp65 cross-linking. OMAR1 (*solid line*) or an irrelevant IgG1 (*dashed line*) was added to NK-92MI cells and, after baseline recording for 30 s, cross-linked by addition of anti-mouse IgG antibodies (*vertical dashed line*). The ratio of median fluorescence intensities (*fluo-4/fura red*) was recorded as a function of time by flow cytometry. One representative of three independent experiments is depicted. *C*, the calcium flux of Jurkat-NKp65, Jurkat-NKp65-N3D, or Jurkat-NKp80-DG cells was assessed upon cross-linking with OMAR1 (*NKp65*) or 5D12 (*NKp80-DG*) as described in *B*.

mass formed by such sNKp65 and sKACL homodimers was readily detectable by size exclusion chromatography (Fig. 5*B*). Next we studied NKp65/KACL interaction by surface plasmon resonance (SPR). The structure of the $(sNKp65)_2$-$(sKACL)_2$ tetrameric complex shows that each NKp65 molecule interacts with one KACL molecule in an identical manner, employing the same interface (16). Therefore, the SPR binding profiles of sNKp65 to immobilized homodimeric sKACL should differ for monomeric *versus* homodimeric sNKp65. In fact, the binding behavior of sNKp65 clearly matched that of a bivalent binding mode, as predicted for homodimeric sNKp65, but not that of a monovalent binding mode, as expected for monomeric sNKp65 (Fig. 5, *C* and *D*). When analyzing the interaction of homodimeric sKACL with immobilized homodimeric NKp65, we also observed a bivalent binding mode well in line with the prediction (Fig. 5, *E* and *F*).

To assess NKp65 signaling upon engagement of the natural ligand KACL, we stimulated NK-92MI-NKp65 cells with sKACL-Fc and analyzed NKp65 immunoprecipitates for NKp65 phosphorylation and Syk recruitment (Fig. 6). NKp65 and NKp65-N3D, but not NKp65-Y7F, became phosphorylated when stimulated with sKACL-Fc, whereas treatment with an irrelevant control protein had no effect. Again, NKp65-N3D showed enhanced phosphorylation compared with NKp65, but neither receptor was able to recruit Syk upon stimulation, well in line with previous results. Together, these results support the notion that NKp65 occurs as a non-disulfide linked homodimer and that the interaction with its ligand KACL is sufficient for NKp65 phosphorylation but does not result in Syk recruitment.

## Discussion

Signaling by activating immunoreceptors is often initiated by the phosphorylation of tyrosine residues embedded in ITAM sequences through Src family kinase (SFK) members with subsequent recruitment and activation of Syk family kinases. For T cells, it was shown that the exclusion of CD45 and enrichment of the SFK Lck upon target cell binding induce phosphotyrosinylation of the T cell receptor and, thereby, initiate signaling (31). It is thought that this initial phosphorylation step is a result of local clustering of receptor and tyrosine kinases as well as an exclusion of tyrosine phosphatases (32). Hence, we started our investigations on NKp65 signaling by examining phosphotyrosinylation of NKp65. Both inhibition of phosphatases as well as NKp65 cross-linking by an NKp65-specific mAb resulted in phosphotyrosinylation of NKp65, demonstrating that either absence of phosphatase activity or NKp65 clustering is sufficient to induce NKp65 phosphotyrosinylation. NKp65 phosphorylation is strictly dependent on tyrosine 7, and, correspondingly, NKp65-Y7F mutants were unable to trigger degranulation and calcium influx. Tyrosine 7 of NKp65 is embedded into a sequence module resembling a hemITAM that was originally described for myeloid-specific CTLRs such as CLEC-2 and Dectin-1 (21, 22). More recently, we found that the CTLR NKp80 expressed by NK cells and a subset of CD8 $\alpha\beta$ T cells and $\gamma\delta$ T cells (11, 33) also transduce activating signals via a cytoplasmic hemITAM-like sequence (27). Of note, NKp80 is the only known hemITAM-bearing receptor of human NK cells and has very recently been reported as a marker of functionally matured, perforin-expressing NK cells (34). Although CLEC-2 and Dectin-1 directly recruit Syk for

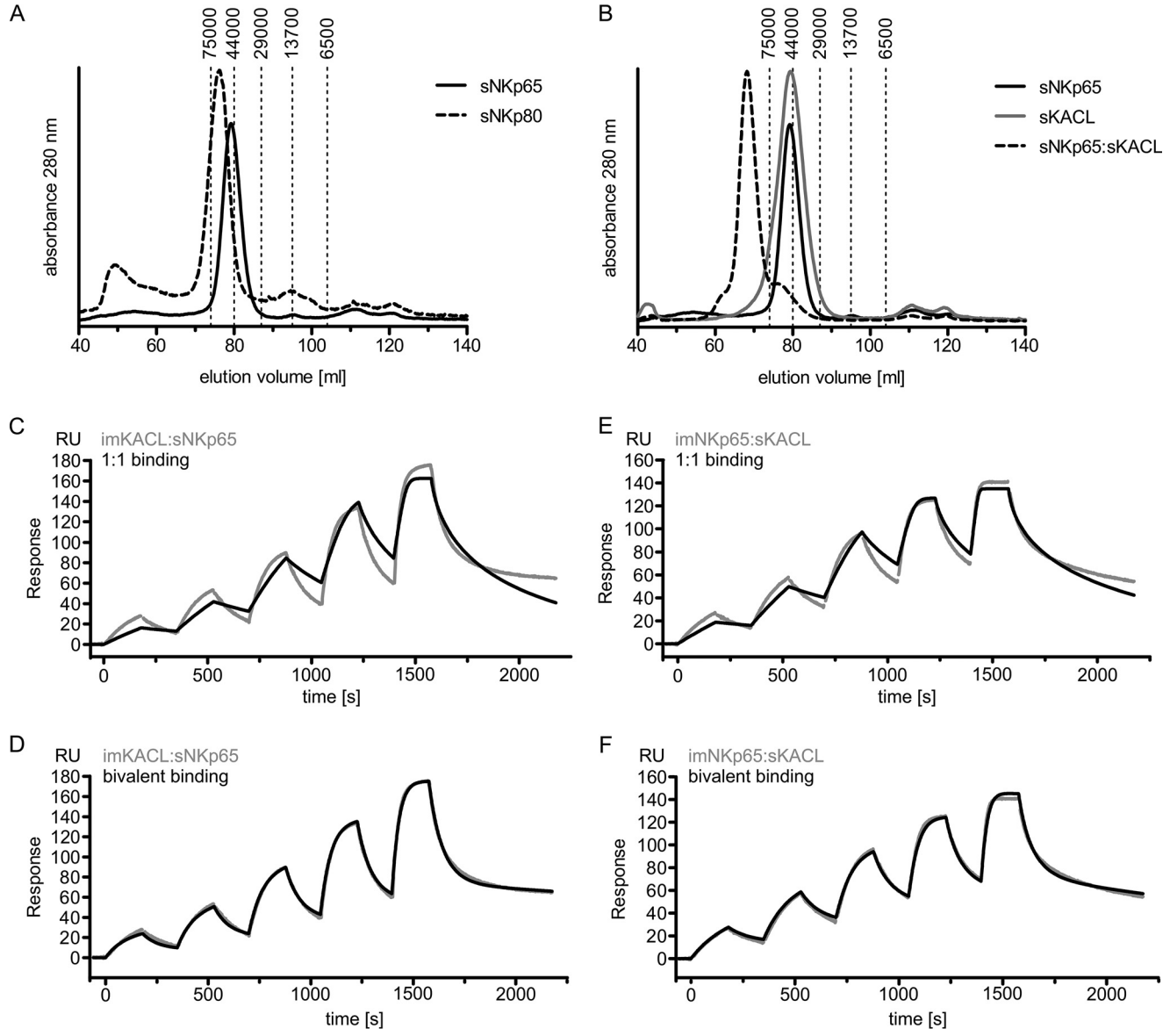


FIGURE 5. **NKp65 forms homodimers in solution and binds to homodimeric KACL in a bivalent binding mode.** *A*, sizing of highly purified soluble ectodomains of NKp65 (*sNKp65*) and NKp80 (*sNKp80*). *B*, complex formation of sNKp65 and sKACL as assessed by gel filtration. *A* and *B*, *dashed vertical lines* indicate elution volumes of proteins used for calibration of the sizing column with molecular masses of the proteins given in daltons. *C–F*, surface plasmon resonance of sKACL and sNKp65. *C* and *D*, biotinylated sKACL was immobilized on a streptavidin sensor chip, and sNKp65 was injected at increasing concentrations (1.25, 2.5, 5, 10, and 20 nM). *E* and *F*, biotinylated sNKp65 was immobilized on a streptavidin sensor chip, and sKACL was injected at increasing concentrations (1.25, 2.5, 5, 10, and 20 nM). Measurements (*gray lines*) were fitted with either a 1:1 binding model (*C* and *E*) or a bivalent binding model (*D* and *F*).

signaling, NKp80 also signals via Syk, but without recruiting Syk directly (28). We now report, for the close NKp80 relative NKp65, Syk-dependent cellular activation without apparent direct Syk recruitment by phosphotyrosinylated NKp65. However, despite these functional parallels, the structural determinants accountable for the impaired Syk recruitment are different for NKp80 and NKp65. In the hemITAM of NKp80, two non-consensus amino acids, glutamic acid 5 and arginine 6, are clearly responsible for the failure to recruit Syk (28), whereas, in NKp65, the hemITAM conforms to the consensus and does not itself appear to be accountable for the impaired Syk recruitment. Hence, we speculate that amino acids located outside of the NKp65 hemITAM may determine the failure to recruit Syk either by conformational changes or by preferential recruitment of other signaling proteins. However, it should be stated that our data do not formally exclude the possibility that an exceptionally low affinity of the Syk SH2 domains for the phosphotyrosinylated NKp65 hemITAM precluded detection of NKp65 in association with Syk for technical reasons.

We had originally reported that NKp65 occurs as a non-disulfide-linked homodimer (12). However, based on the crystal structure of the NKp65-KACL complex, it was suggested that NKp65 molecules occur as monomers and bind as such to KACL homodimers (16). Hence, we readdressed this issue to assess whether the monomeric occurrence of NKp65 may be accountable for its signaling mechanism. However, both gel filtration and SPR strongly support our original notion that NKp65 molecules occur as homodimers interacting with

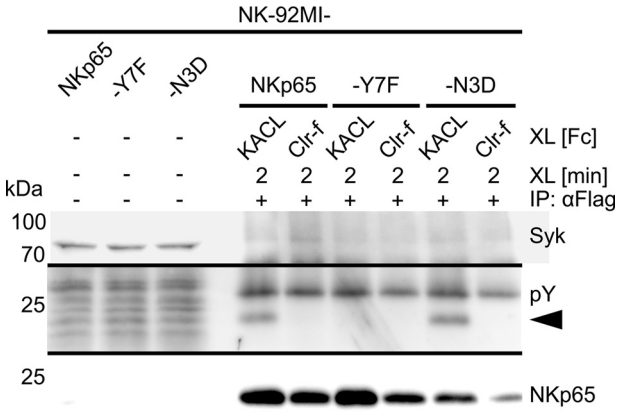


FIGURE 6. **KACL binding induces NKp65 phosphotyrosinylation but not Syk recruitment.** NKp65 on NK-92MI-NKp65, NK-92MI-NKp65-Y7F, or NK-92MI-NKp65-N3D was cross-linked (*XL*) by addition of sKACL-Fc and secondary anti-human IgG-Fc antibodies for 2 min at 37 °C. For control, sClr-f-Fc was added instead of sKACL-Fc. Subsequently, NKp65 was immunoprecipitated from cellular lysates with anti-FLAG mAb M2, and immunoprecipitates were probed for the presence of Syk with mAb 4D10.2 (*top*) and for phosphotyrosinylation of NKp65 with the anti-phosphotyrosine mAb 4G10 (*center*). Successful immunoprecipitation of NKp65 was monitored by reprobing the membrane with anti-FLAG mAb M2 (*bottom*). Depicted is one representative of two independent experiments. Phosphorylated NKp65 is marked by an *arrowhead*.

homodimeric KACL in a manner similar to the related receptor ligand pairs NKp80-AICL and NKR-P1A-LLT1.

The triacidic motif of the hemITAM is slightly altered in NKp65, with an asparagine replacing aspartic acid (Fig. 1*C*). Mutational studies of the hemITAM receptor CLEC-2 expressed on platelets and neutrophils (35) showed that phosphotyrosinylation and signaling depend on the triacidic motif (23). Also, the binding of Syk-SH2 domains to phosphorylated peptides in which the triacidic motif of CLEC-2 was substituted by alanine residues is reduced 3- to 4-fold (23). In the absence of any other obvious sequence substitutions in NKp65, we speculated that the altered triacidic motif in NKp65 may be the reason for the observed lack of Syk recruitment. However, reconstitution of the triacidic motif in the NKp65 hemITAM did not reconstitute Syk recruitment, although it led to a profound increase in hemITAM phosphorylation well in line with the sequence preferences of the catalytic domain of Src kinases (36). These observations were consistent and made independently of the way of NKp65 cross-linking (antibody or ligand) and of the cell line (NK-92MI or Jurkat).

Upon ligand engagement by CLEC-2, phosphorylation of the hemITAM has mainly been attributed to the activity of Syk (25, 37). In contrast, hemITAM phosphotyrosinylation of NKp80 solely depends on SFK but not on Syk activity (28), correlating with the failure to recruit Syk. Because NKp65 also does not recruit Syk, we expect that the mechanism underlying NKp65 hemITAM phosphorylation rather resembles that of NKp80 than that of CLEC-2. In Jurkat cells, the calcium flux stimulated by NKp65 was markedly time-delayed compared with NK-92MI cells, whereas the NKp80-DG-induced calcium flux was comparable in both cell lines. Because both cell lines express comparable levels of Syk and ZAP-70 (data not shown), this difference cannot be attributed to the Syk family members. Rather, the delayed NKp65 calcium flux in Jurkat cells is reminiscent of Lyn-negative DT40 cells showing a time-delayed B cell receptor (BCR)-induced calcium flux compared with the wild-type cell line (38). SFK members can have distinct functions, as they differentially recognize specific phosphoproteins (39). Hence, NKp65 signaling may require a specific SFK member that is differentially expressed in NK-92MI *versus* Jurkat cells. It is known that SFK can occur as specific constitutive complexes with certain receptors (40), and it remains to be shown whether NKp80 or NKp65 phosphotyrosinylation depends on certain SFKs. For example, both Blk and Lyn, but not Fyn, are capable to bind Syk in B cells (41).

In summary, cellular activation by NKp65 strictly depends on the NKp65 hemITAM and Syk activity. The failure to detect a recruitment of Syk to phosphorylated NKp65 suggests that the NKp65 hemITAM associates with another SH2 domain-bearing protein, subsequently leading to downstream Syk activation. However, it cannot be formally excluded that Syk binds NKp65 with an exceptionally low affinity following NKp65-KACL interaction. Further studies will have to address these issues, especially in the context of cells physiologically expressing NKp65, which remains to be identified.

## Experimental Procedures

*Antibodies and Recombinant Proteins*—NKp80 mAb 5D12 was described previously (11). NKp65 mAb OMAR1 was obtained by immunizing mice with NKp65-transfected P815 cells.[3] HRP-conjugated anti-Tyr(P) (clone P-100), anti-Syk (2712), and anti-pSyk (Tyr-525/526, 2710) were purchased from Cell Signaling Technology (Danvers, MA). HRP-conjugated anti-Tyr(P) (clone 4G10) was from Merck Millipore (Billerica, MA). Purified and biotin-conjugated anti-FLAG M2 antibody was purchased from Sigma-Aldrich (St. Louis, MO), anti-Syk (clone 4D10.2) from BioLegend (San Diego, CA), sheep anti-NKp80 from R&D Systems (Minneapolis, MN), anti-CD56-PE (clone N901) from Beckman Coulter (Brea, CA), and anti-CD107a-APC (clone H4A3) from BD Biosciences. All secondary antibodies were purchased from Jackson ImmunoResearch Laboratories (Newmarket, UK). Soluble ectodomains of KACL, AICL, NKp65, and NKp80 were purified from 293T supernatants and biotinylated using BirA ligase as described previously (11, 12). Fusion proteins of the extracellular parts of KACL (Ala-47 to Leu-174) and Clr-f (Val-73 to Val-218) with an amino-terminal human Fc fragment were cloned into pFUSE-hIgG1-FcEQ (42) (a kind gift from Joachim Koch, University of Mainz) and purified from 293T supernatants by protein A-agarose (Bio-Rad).

*Cells and Cellular Transduction*—NK-92MI cells (14) were cultured in Iscove's modified Dulbecco's medium (Sigma-Aldrich) with 10% FCS (Biochrom, Berlin, Germany) and 10% horse serum (Sigma-Aldrich) and Jurkat cells in RPMI 1640 medium (Sigma-Aldrich) with 10% FCS. Coding sequences of NKp80 and NKp65 were cloned into pMXsIP (kindly provided by Toshio Kitamura, University of Tokyo). NKp65-N3D cDNA was generated by inverse vector PCR using Phusion polymerase (New England Biolabs, Ipswich, UK) with mutation-containing primers followed by blunt end ligation. Retroviruses were pro-

[3] I. Vogler *et al.*, manuscript in preparation.

duced using Phoenix Ampho cells for transduction of NK-92MI and Jurkat cells according to standard protocols as described previously (27). NK-92MI and Jurkat cells stably expressing NKp80 or NKp65 were selected using puromycin at 5.0 and 0.6 μg/ml, respectively.

*Flow Cytometry, Degranulation, and Calcium Flux*—For extracellular staining, cells were washed with ice-cold FACS buffer (PBS, 2% FCS, 2 mM EDTA, and 0.01% sodium azide) and incubated with antibodies for 20 min on ice, followed by washing and incubation with an appropriate fluorochrome-conjugated secondary antibody and washing. Dead cells were excluded by DAPI staining. For permeabilized staining, cells were first stained with the fixable viability dye eFluor450 (eBioscience, San Diego, CA), followed by fixation and permeabilization (Cytofix/Cytoperm, BD Biosciences). Antibody incubation and washing steps were performed in saponin buffer (PBS, 0.1% saponin, 0.5% BSA, and 0.01% sodium azide). Flow cytometric data were acquired using a FACSCanto II (BD Biosciences) and analyzed using FlowJo (Tree Star, Ashland, OR). Degranulation of NK-92MI cells was monitored by CD107a surfacing after 2-h co-culture with P815 preincubated with 10 μg/ml mAb for 5 min at room temperature (final concentration, 3.33 μg/ml) or PMA (250 ng/ml) and ionomycin (1 μM) as positive controls (both from Sigma-Aldrich) in the presence of anti-CD107a-APC and Golgi-Stopp (both from BD Biosciences). For calcium flux measurements by flow cytometry, $1 \times 10^6$ cells resuspended in 100 μl of Hanks' balanced salt solution with calcium and magnesium (HBSS, Thermo Scientific, Rockford, IL) were loaded with 10 μg/ml mAb for 30 min on ice. Then, 300 μl of dye loading buffer (HBSS, 2 μM fluo-4, 5 μM fura red, and 2 mM probenecid (Thermo Scientific)) was added, and cells were incubated for 30 min at 30 °C. After washing, cells were resuspended in 300 μl of HBSS and prewarmed to 37 °C for 5 min. DAPI was added shortly before the measurement, and the ratio of fluo-4/fura red was acquired over time. First, the baseline was acquired for 30 s. Then, the tube was briefly removed from the cytometer to add 4 μg of $F(ab)_2$ fragment of goat anti-mouse IgG antibody, and the acquisition continued for 210 s. Data were analyzed using FlowJo by plotting the ratio of the median fluorescence intensity *versus* time.

*Antibody-mediated Cross-linking, Immunoprecipitation, and Immunoblotting*—Cells were resuspended in Iscove's modified Dulbecco's medium at $2 \times 10^7$ cells/ml and loaded with 10 μg/ml mAb for 30 min on ice. After washing, cells were resuspended at $1 \times 10^8$ cells/ml and prewarmed for 1 min at 37 °C. Then, 60 μg/ml goat anti-mouse IgG $F(ab)_2$ fragment-specific antibody was added, cells were incubated further at 37 °C, and the reaction was stopped by addition of ice-cold lysis buffer (20 mM Tris/HCl (pH 7.5), 140 mM NaCl, 5 mM EDTA, 1.1% Nonidet P-40, Complete phosphatase inhibitor mixture (Roche), 10 mM $Na_4P_2O_7$, 10 mM NaF, and 1 mM $Na_3VO_4$). Lysis was performed for 20 min on ice, and lysates were cleared by centrifugation for 15 min at 17,000 × *g* and 4 °C. For immunoprecipitation, protein A/G magnetic beads (Thermo Scientific) were preloaded with 3–10 μg of mAb/25 μl of beads, and, after washing, beads and cleared lysates were mixed and incubated for 3 h at 4 °C on a rotator. Beads were washed four times with wash buffer (20 mM Tris/HCl (pH 7.5), 140 mM NaCl, 5 mM EDTA, 1.1% Nonidet P-40), and proteins were eluted by addition of 1.5× denaturing buffer (New England Biolabs) and boiling at 95 °C for 10 min. PNGaseF (New England Biolabs) digestion was performed according to the protocol of the manufacturer. Proteins were separated by standard SDS-PAGE, followed by tank blotting onto a PVDF membrane (Carl Roth, Karlsruhe, Germany). Blots were then blocked with TBS containing 0.1% Tween 20 (Applichem) and 5% BSA for phosphoblots or 5% milk powder for all others, incubated with primary and HRP-conjugated secondary antibodies, and developed by enhanced chemiluminescence using West Pico (Thermo Scientific) or HRP-Juice Plus (PJK, Kleinbittersdorf, Germany).

*GST Pulldown*—The tandem SH2 domains of human Syk were cloned from NK-92MI cDNA into pGEX-4T1 with the primers described previously (43) and expressed in *Escherichia coli* BL21 at 30 °C for 16 h in autoinduction medium. Cells were lysed using pulldown lysis buffer (Thermo Scientific), and the GST fusion protein was purified with glutathione-agarose (Thermo Scientific) according to the instructions of the manufacturer. After elution with 10 mM glutathione (Thermo Scientific) and dialysis, the GST fusion protein was immobilized on glutathione-agarose. NK-92MI cells stably expressing NKp65, NKp65-Y7F, NKp80-DG, or NKp80 were treated with 2 mM pervanadate for 5 min and lysed as described. FLAG-tagged receptors were immunoprecipitated with M2 magnetic beads and eluted with 150 ng/μl 3× FLAG-peptide (both from Sigma-Aldrich). The enriched receptors were applied to the immobilized GST fusion protein. Beads were washed five times with wash buffer (20 mM Tris/HCl (pH 7.5), 140 mM NaCl, 5 mM EDTA, and 0.55% Nonidet P-40) and eluted using 1.5× denaturing buffer (New England Biolabs) and boiling at 95 °C for 10 min. PNGaseF (New England Biolabs) digestion was performed according to the protocol of the manufacturer.

*Gel Filtration and Surface Plasmon Resonance*—Proteins were loaded onto a HiLoad 16/60 Superdex 200 gel filtration column at a flow rate of 0.5 ml/min. The Gel Filtration LMW Calibration Kit (GE Healthcare) was employed for column calibration according to the protocol of the manufacturer. Surface plasmon resonance was performed on a Biacore X100 (GE Healthcare) utilizing the Biotin CAPture kit (GE Healthcare) according to the protocol of the manufacturer.

*Statistical Analysis and Protein Sequence Alignment*—Statistical analysis and data presentation were performed using Prism 5 (GraphPad, San Diego, CA). Sequences were aligned using ClustalX (44).

*Author Contributions*—B. B. planned and performed most of the experiments, analyzed the data, and wrote the manuscript. T. W. performed immunoprecipitation and immunoblotting and calcium flux. T. Z. performed surface plasmon resonance. E. R. produced the KACL and Clr-f-Fc fusion proteins. A. S. conceptualized the research, analyzed the data, and wrote the manuscript.

*Acknowledgment—We thank Dr. Stefan Leibelt for help with the gel filtration assays.*

## References


1. Diefenbach, A., Colonna, M., and Koyasu, S. (2014) Development, differentiation, and diversity of innate lymphoid cells. *Immunity* **41,** 354–365
2. Eberl, G., Colonna, M., Di Santo, J. P., and McKenzie, A. N. (2015) Innate lymphoid cells. Innate lymphoid cells: a new paradigm in immunology. *Science* **348,** aaa6566
3. Waldhauer, I., and Steinle, A. (2008) NK cells and cancer immunosurveillance. *Oncogene* **27,** 5932–5943
4. Cerwenka, A., and Lanier, L. L. (2016) Natural killer cell memory in infection, inflammation and cancer. *Nat. Rev. Immunol.* **16,** 112–123
5. Hao, L., Klein, J., and Nei, M. (2006) Heterogeneous but conserved natural killer receptor gene complexes in four major orders of mammals. *Proc. Natl. Acad. Sci. U.S.A.* **103,** 3192–3197
6. Vogler, I., and Steinle, A. (2011) Vis-a-vis in the NKC: genetically linked natural killer cell receptor/ligand pairs in the natural killer gene complex (NKC). *J. Innate. Immun.* **3,** 227–235
7. Bartel, Y., Bauer, B., and Steinle, A. (2013) Modulation of NK cell function by genetically coupled C-type lectin-like receptor/ligand pairs encoded in the human natural killer gene complex. *Front Immunol.* **4,** 362
8. Aldemir, H., Prod'homme, V., Dumaurier, M. J., Retiere, C., Poupon, G., Cazareth, J., Bihl, F., and Braud, V. M. (2005) Cutting edge: lectin-like transcript 1 is a ligand for the CD161 receptor. *J. Immunol.* **175,** 7791–7795
9. Rosen, D. B., Bettadapura, J., Alsharifi, M., Mathew, P. A., Warren, H. S., and Lanier, L. L. (2005) Cutting edge: lectin-like transcript-1 is a ligand for the inhibitory human NKR-P1A receptor. *J. Immunol.* **175,** 7796–7799
10. Vitale, M., Falco, M., Castriconi, R., Parolini, S., Zambello, R., Semenzato, G., Biassoni, R., Bottino, C., Moretta, L., and Moretta, A. (2001) Identification of NKp80, a novel triggering molecule expressed by human NK cells. *Eur. J. Immunol.* **31,** 233–242
11. Welte, S., Kuttruff, S., Waldhauer, I., and Steinle, A. (2006) Mutual activation of natural killer cells and monocytes mediated by NKp80-AICL interaction. *Nat. Immunol.* **7,** 1334–1342
12. Spreu, J., Kuttruff, S., Stejfova, V., Dennehy, K. M., Schittek, B., and Steinle, A. (2010) Interaction of C-type lectin-like receptors NKp65 and KACL facilitates dedicated immune recognition of human keratinocytes. *Proc. Natl. Acad. Sci. U.S.A.* **107,** 5100–5105
13. Klimosch, S. N., Bartel, Y., Wiemann, S., and Steinle, A. (2013) Genetically coupled receptor-ligand pair NKp80-AICL enables autonomous control of human NK cell responses. *Blood* **122,** 2380–2389
14. Gong, J. H., Maki, G., and Klingemann, H. G. (1994) Characterization of a human cell line (NK-92) with phenotypical and functional characteristics of activated natural killer cells. *Leukemia* **8,** 652–658
15. Spreu, J., Kienle, E. C., Schrage, B., and Steinle, A. (2007) CLEC2A: a novel, alternatively spliced and skin-associated member of the NKC-encoded AICL-CD69-LLT1 family. *Immunogenetics* **59,** 903–912
16. Li, Y., Wang, Q., Chen, S., Brown, P. H., and Mariuzza, R. A. (2013) Structure of NKp65 bound to its keratinocyte ligand reveals basis for genetically linked recognition in natural killer gene complex. *Proc. Natl. Acad. Sci. U.S.A.* **110,** 11505–11510
17. Bauer, B., Spreu, J., Rohe, C., Vogler, I., and Steinle, A. (2015) Key residues at the membrane-distal surface of KACL, but not glycosylation, determine the functional interaction of the keratinocyte-specific C-type lectin-like receptor KACL with its high-affinity receptor NKp65. *Immunology* **145,** 114–123
18. Vivier, E., Nunès, J. A., and Vély, F. (2004) Natural killer cell signaling pathways. *Science* **306,** 1517–1519
19. Lanier, L. L. (2008) Up on the tightrope: natural killer cell activation and inhibition. *Nat. Immunol.* **9,** 495–502
20. Orange, J. S. (2008) Formation and function of the lytic NK-cell immunological synapse. *Nat. Rev. Immunol.* **8,** 713–725
21. Fuller, G. L., Williams, J. A., Tomlinson, M. G., Eble, J. A., Hanna, S. L., Pöhlmann, S., Suzuki-Inoue, K., Ozaki, Y., Watson, S. P., and Pearce, A. C. (2007) The C-type lectin receptors CLEC-2 and Dectin-1, but not DC-SIGN, signal via a novel YXXL-dependent signaling cascade. *J. Biol. Chem.* **282,** 12397–12409
22. Sancho, D., and Reis e Sousa. (2012) Signaling by myeloid C-type lectin receptors in immunity and homeostasis. *Annu. Rev. Immunol.* **30,** 491–529
23. Hughes, C. E., Sinha, U., Pandey, A., Eble, J. A., O'Callaghan, C. A., and Watson, S. P. (2013) Critical role for an acidic amino acid region in platelet signaling by the HemITAM (hemi-immunoreceptor tyrosine-based activation motif) containing receptor CLEC-2 (C-type lectin receptor-2). *J. Biol. Chem.* **288,** 5127–5135
24. Hughes, C. E., Pollitt, A. Y., Mori, J., Eble, J. A., Tomlinson, M. G., Hartwig, J. H., O'Callaghan, C. A., Fütterer, K., and Watson, S. P. (2010) CLEC-2 activates Syk through dimerization. *Blood* **115,** 2947–2955
25. Séverin, S., Pollitt, A. Y., Navarro-Nuñez, L., Nash, C. A., Mourão-Sá, D., Eble, J. A., Senis, Y. A., and Watson, S. P. (2011) Syk-dependent phosphorylation of CLEC-2: a novel mechanism of hem-immunoreceptor tyrosine-based activation motif signaling. *J. Biol. Chem.* **286,** 4107–4116
26. Manne, B. K., Badolia, R., Dangelmaier, C., Eble, J. A., Ellmeier, W., Kahn, M., and Kunapuli, S. P. (2015) Distinct pathways regulate Syk protein activation downstream of immune tyrosine activation motif (ITAM) and hemITAM receptors in platelets. *J. Biol. Chem.* **290,** 11557–11568
27. Dennehy, K. M., Klimosch, S. N., and Steinle, A. (2011) Cutting edge: NKp80 uses an atypical hemi-ITAM to trigger NK cytotoxicity. *J. Immunol.* **186,** 657–661
28. Rückrich, T., and Steinle, A. (2013) Attenuated natural killer (NK) cell activation through C-type lectin-like receptor NKp80 is due to an anomalous hemi-immunoreceptor tyrosine-based activation motif (HemITAM) with impaired Syk kinase recruitment capacity. *J. Biol. Chem.* **288,** 17725–17733
29. Kerrigan, A. M., and Brown, G. D. (2010) Syk-coupled C-type lectin receptors that mediate cellular activation via single tyrosine based activation motifs. *Immunol. Rev.* **234,** 335–352
30. Suzuki-Inoue, K., Fuller, G. L., García, A., Eble, J. A., Pöhlmann, S., Inoue, O., Gartner, T. K., Hughan, S. C., Pearce, A. C., Laing, G. D., Theakston, R. D., Schweighoffer, E., Zitzmann, N., Morita, T., Tybulewicz, V. L., *et al.* (2006) A novel Syk-dependent mechanism of platelet activation by the C-type lectin receptor CLEC-2. *Blood* **107,** 542–549
31. Chang, V. T., Fernandes, R. A., Ganzinger, K. A., Lee, S. F., Siebold, C., McColl, J., Jönsson, P., Palayret, M., Harlos, K., Coles, C. H., Jones, E. Y., Lui, Y., Huang, E., Gilbert, R. J., Klenerman, D., *et al.* (2016) Initiation of T cell signaling by CD45 segregation at "close contacts." *Nat. Immunol.* **17,** 574–582
32. Davis, S. J., and van der Merwe, P. A. (2006) The kinetic-segregation model: TCR triggering and beyond. *Nat. Immunol.* **7,** 803–809
33. Kuttruff, S., Koch, S., Kelp, A., Pawelec, G., Rammensee, H. G., and Steinle, A. (2009) NKp80 defines and stimulates a reactive subset of CD8 T cells. *Blood* **113,** 358–369
34. Freud, A. G., Keller, K. A., Scoville, S. D., Mundy-Bosse, B. L., Cheng, S., Youssef, Y., Hughes, T., Zhang, X., Mo, X., Porcu, P., Baiocchi, R. A., Yu, J., Carson, W. E., 3rd, and Caligiuri, M. A. (2016) NKp80 defines a critical step during human natural killer cell development. *Cell Rep.* **16,** 379–391
35. Kerrigan, A. M., Dennehy, K. M., Mourão-Sá, D., Faro-Trindade, I., Willment, J. A., Taylor, P. R., Eble, J. A., Reis e Sousa, C., and Brown, G. D. (2009) CLEC-2 is a phagocytic activation receptor expressed on murine peripheral blood neutrophils. *J. Immunol.* **182,** 4150–4157
36. Songyang, Z., Carraway, K. L., 3rd, Eck, M. J., Harrison, S. C., Feldman, R. A., Mohammadi, M., Schlessinger, J., Hubbard, S. R., Smith, D. P., and Eng, C. (1995) Catalytic specificity of protein-tyrosine kinases is critical for selective signalling. *Nature* **373,** 536–539
37. Spalton, J. C., Mori, J., Pollitt, A. Y., Hughes, C. E., Eble, J. A., and Watson, S. P. (2009) The novel Syk inhibitor R406 reveals mechanistic differences in the initiation of GPVI and CLEC-2 signaling in platelets. *J. Thromb. Haemost.* **7,** 1192–1199
38. Takata, M., Sabe, H., Hata, A., Inazu, T., Homma, Y., Nukada, T., Yamamura, H., and Kurosaki, T. (1994) Tyrosine kinases Lyn and Syk regulate B cell receptor-coupled $Ca^{2+}$ mobilization through distinct pathways. *EMBO J.* **13,** 1341–1349

39. Malek, S. N., and Desiderio, S. (1993) SH2 domains of the protein-tyrosine kinases Blk, Lyn, and Fyn(T) bind distinct sets of phosphoproteins from B lymphocytes. *J. Biol. Chem.* **268,** 22557–22565
40. Rajasekaran, K., Kumar, P., Schuldt, K. M., Peterson, E. J., Vanhaesebroeck, B., Dixit, V., Thakar, M. S., and Malarkannan, S. (2013) Signaling by Fyn-ADAP via the Carma1-Bcl-10-MAP3K7 signalosome exclusively regulates inflammatory cytokine production in NK cells. *Nat. Immunol.* **14,** 1127–1136
41. Aoki, Y., Kim, Y. T., Stillwell, R., Kim, T. J., and Pillai, S. (1995) The SH2 domains of Src family kinases associate with Syk. *J. Biol. Chem.* **270,** 15658–15663
42. Hartmann, J., Tran, T. V., Kaudeer, J., Oberle, K., Herrmann, J., Quagliano, I., Abel, T., Cohnen, A., Gatterdam, V., Jacobs, A., Wollscheid, B., Tampé, R., Watzl, C., Diefenbach, A., and Koch, J. (2012) The stalk domain and the glycosylation status of the activating natural killer cell receptor NKp30 are important for ligand binding. *J. Biol. Chem.* **287,** 31527–31539
43. Yanaga, F., Poole, A., Asselin, J., Blake, R., Schieven, G. L., Clark, E. A., Law, C. L., and Watson, S. P. (1995) Syk interacts with tyrosine-phosphorylated proteins in human platelets activated by collagen and cross-linking of the Fc γ-IIA receptor. *Biochem. J.* **311,** 471–478
44. Larkin, M. A., Blackshields, G., Brown, N. P., Chenna, R., McGettigan, P. A., McWilliam, H., Valentin, F., Wallace, I. M., Wilm, A., Lopez, R., Thompson, J. D., Gibson, T. J., and Higgins, D. G. (2007) ClustalW and ClustalX version 2.0. *Bioinformatics* **23,** 2947–2948